Thermo-physico-chemical and statistical mechanical properties of Washingtonian filifera new lignocellulosic fiber

Djamel Edinne Gaagaia[a,b*], Mustapha Bouakba[a] and Abdelheq Layachi[c,d]

[a]Department of Mechanical Engineering, Faculty of Applied Sciences, University of Kasdi Merbah Ouargla, 30000, Algeria
[b]Research Center in Industrial Technologies CRTI, p.o.box 64, Cheraga, Algeria
[c]Laboratoire des Silicates, Polymères et Nanocomposites (LSPN) Université 08 mai 1945, 24000 Guelma, Algeria
[d]Université des Frères Mentouri Constantine 1(ISTA), Algérie

A R T I C L E I N F O	A B S T R A C T
	In this work, novel cellulosic fibers are extracted from Washingtonia Filifera (WF) plant using an environment friendly technique. Morphological, physico-chemical, thermal and mechanical properties are reported in this paper. Micro graphical SEM shows the presence of cells in the fiber. FTIR and XRD experimental analyzes show a cristinality index of 48.88%, and the WF fibers are found to be thermally stable until 201°C by using TGA and DTG thermo graphic analyzes with an appropriate activation energy of 72.46 kJ/mol, where Young modulus and tensile strength of strain were determined using tensile tests of single fiber at 2.17 GPa, 134 MPa and 26.55%, respectively. Mechanical properties are analyzed using a statistical method.

1. Introduction

Nowadays, the usage of natural fibers as reinforcement in polymer matrix based composites is the subject of interest of many researchers around the globe mainly due to climate change concerns, greenhouse effect, deforestation, non-degradable waste in addition to air and water pollution that are becoming the main preoccupations of the entire humanity (Ishak et al., 2013). Natural fibers have many advantages that made them attractive with respect to synthetic fibers such as their lightweight, disponibility (Guo et al., 2013), their renewable aspect, biodegradability, non-corrosive aspect, their high specific module, high rigidity, ecological nature in addition to their low cost (Jawaid et al., 2011). These are the main reasons for the usage of vegetable cellulosic fibers in industrial applications. Such properties of natural fibers when used as reinforcement in composite materials have attracted the attention of many research works (Liu et al., 2018; Baskaran el at., 2018; Aliha et al., 2017). The fibers of vegetables include tow fibers or solid fibers, seeds, fruits, wood, straw and other herbal fibers. Firstly, existing classical natural fibers such as cassava (Teixeira et al., 2009), chanvre (Keller, 2013), lin (Thomason, 2008), Diss (Mustapha et al., 2016), Banana (Ibrahim et al., 2010), etc. are found. With the continuity of the technological development of composite materials, researchers have discovered

novel fibers in the nature that have the same advantages such as Native African Napier Grass (Reddy et al., 2018), Furcraea foetida (Manimaran et al., 2018), Aegle marmelos (Sandeep et al., 2017). Natural fibers are considered as natural composites composed mainly of cellulose fibrils (fibers) incorporated in the lignin matrix (resin). This cellulosic fibrils are aligned along the fiber regardless of its origin, e.g. if it is extracted from the bark or stem, from leaves or fruits (Suryanto et al., 2013). Several recent studies were done on the subject of novel lignocellulosic fibers. Morphological characterization, physic-chemical properties, mechanical and thermal such as, Cactus (Bouakba et al., 2013), Dichrostachys Cinerea (Baskaran et al., 2018) and Arundo donax L leaf fibers (Scalici et al., 2016).

The objective of this work is the introduction of a novel fiber extracted from the vegetable Washingtonia Filifera (WF), which have been the subject of few physico-chemical and mechanical characterizations for the purpose of the development of bio-composite materials reinforced by this fiber. Its response and characteristics are compared with other lignocellulosic fibers existing in the literature. To the extent knowledge of the authors, the reinforcement of bio-composite materials using lignocellulosic fiber is proposed for the first time. For this purpose, morphological and physic-chemical characteristics of WF fibers are examined using scanning electronic microscope (SEM), X-ray diffraction (XRD) and fourier-transform infrared spectroscopy (FTIR). Furthermore, mechanical characterizations for tensile test of the WF fibers are executed. Finally, results are processed using statistical analysis with two Weibull parameters.
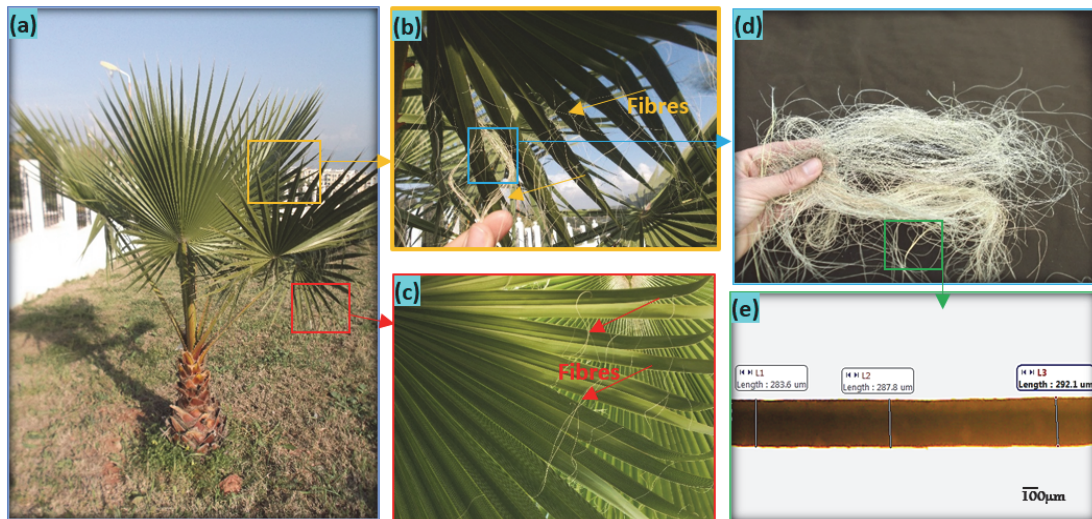

Fig.1. (a) Washingtonian Filifera plant, (b, c) Washingtonian Filifera leaf and fibers, (d) obtained fibers and (e) optical microscopic image of single fiber of WF

2. Experimental techniques

2.1 Materials

2.1.1 Washingtonia Filifera fibers

Washingtonia Filifera, petticoat palm or California palm, is a palm species (Arecaceae familly) belonging to the family Washingtonia. Its origins are from the Sounth-West of the USA (California, south-west of Arizona) and north-west of Mexico, where it is developed in colonies, in the canyons of arid regions. This type of petticoat palm grows to 23m in height, and it is widely grown in the forest located in the region of Skikda (Algeria). Firstly, the fibers are easily extracted manually and immersed in distilled water for cleaning the surface of the fiber (see Fig. 1). Next, the fibers are stored in a hot air oven for 24 hours at 105°C to remove moisture.

2.1.2 Density of fiber

We use a water pycnometer that has been thoroughly cleaned and wiped. This pycnometer is filled to the mark with water permuted at 20°C, and the weight of the pycnometer filled with water is noted M3. We drain about half of the water in the pycnometer. A mass of 5g of clay powder noted M4 is introduced in the pycnometer. We fill the remaining volume of the pycnometer (containing the clay powder) with permuted water to the mark by adjusting with a syringe. After resetting the scale, we weigh the all and note the mass M5. The Eq. (1) gives the value of the density.

$$d = \left(\frac{M4}{M3 + M4 - M5} * \rho_{eau} \right) \tag{1}$$

with:

$$\rho_{eau} = 1 g/cm^3$$

to analyze the density on the WF fiber, it is observed that the greatest deformation of the order of 26.55 ± 8.24% was obtained for the microfibril angle and 41° and almost like the study carried by (Beakou et al. 2008) who finds that the micro angle fibers 40°, In this context (Azwa et al., 2013) reported that the greatest ductility is provided by the larger angles.

2.3. Thermo-physicochemical characterization

2.3.1 Optical and scanning electron microscopy

The diameter of the single W. Filifera fibers is observed using ZEISS optical microscope equipped with a Moticam 2500 camera digitally controlled by Motic Images Plus V2.0 image processing program. The fibers revealed variation in diameter throughout its length as shown in Fig.1(e). Ten measurements have been taken all along the fiber in different places. The apparent cross-sectional area of each fiber is then calculated from the mean fiber diameter considered a circular. This method, as it was considered a reasonable approximation to study of the natural fibers. The surface of the single W. Filifera fiber, and cross-section were analyzed using a JSM-7600F scanning electron microscope (SEM). To make the fibers and yarns conductive, the samples were sputter-coated with a thin layer of gold. The SEM image was operated at an accelerating voltage of 10 kV, as shown in Fig. 5.

2.3.2 Fourier-transform infrared Spectroscopy (FTIR)

FTIR test is carried out using Shimadzu FTIR-8400S spectrum and its quantitative analysis software. The infrared spectroscopy technique allows the determination of the chemical nature of the analyzed product by identifying some absorption bands present in the spectrum. The vegetable fibers samples are measured on this equipment in a KBr matrix with a scan rate of 32 acquisitions between 500 and 4000 cm^{-1} and a resolution of 2 cm^{-1}.

2.3.3 X-ray diffraction (XRD)

X-ray diffraction measurements are performed on Ultima IV Multipurpose X-Ray Diffractometer XRD, using the spectral line Cu-Kα with a wavelength λ= 1.54056 Å. The X-ray source is a ceramic tube provided with a copper anode and powered by a 40kV voltage and an intensity of 40 mA. The spectrum is recorded between 10° and 30°, each scan is performed with a step of 0.18°.

2.3.4 Thermogravimetric analysis (TGA)

In our study, the thermal analysis namely Thermogravimetry (TG) is performed on a Perkin Elmer TGA-7 with a heating rate of 10°C/min in a nitrogen atmosphere (N$_2$), and for that of cooling is 20

°C/min. The samples were tested in a range between 20°C and 450°C. The masses of the samples used in this work vary from 10-15mg with flow rate 60mL.min^{-1}. The sample is placed in an Al_2O_3.

2.4 .Mechanical characterization

2.4.1. Tensile testing

Due to the variability of vegetable fibers, more than 30 fiber bundles were selected and tested on Zwick/Roell 005Z machine, this machine is equipped with a 5kN force sensor and an integrated linear sensor for the measurement of the displacement of the cross. The machine is controlled by Test expert II software which allows recording the results on a test report. Quasi-static tensile tests on WF cellulosic fibers are tested with a gauge length (GL) of 40 mm according to ASTM D3822-07. These tests were carried out at an ambient temperature of 26°C, and a hygrometry of approximately 55% with a constant speed of 1mm/min. The tests are conducted according to ASTM D638 for the tensile tests.

3. Results and discussions

3.1 SEM analysis

In the testing of the Micrography (SEM), Figure 2(a-d) shows the morphology of WF fibers. Fig. 2 (a, b) shows a longitudinal view of the fiber which presents a non-degraded rough surface suitable for good bonding with the matrix polymer. Fig. 2 (b) shows the zoom of Fig. 2 (a) with X1000 magnification. It can clearly be seen from Fig. 2 (c, d) that the fiber bundles contain aligned fiber cells bound together by lignin and hemicellulose (Beloudeh et al., 2015; Reddy et al., 2014; Fiore et al., 2014).
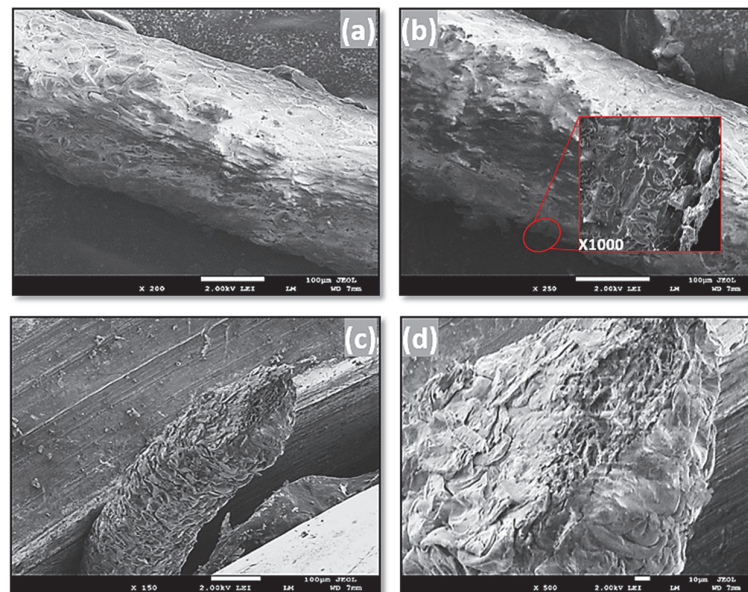

Fig.2. SEM micrographs of (a) longitudinal view of WF fiber and (b) correspond to a zoom longitudinal (c) view the cross-section and (d) correspond to a zoom of the cross section

3.2 Fourier Transform Infrared Spectroscopy

An infrared spectroscopy study is carried out to study the influence of different media on the chemical composition of the fibers. The functions most frequently encountered in the study of polysaccharides

by infrared spectrometry are shown in Table 1. The infrared spectrum of washingtonia Filifera fibers are given in Fig. 3(a).
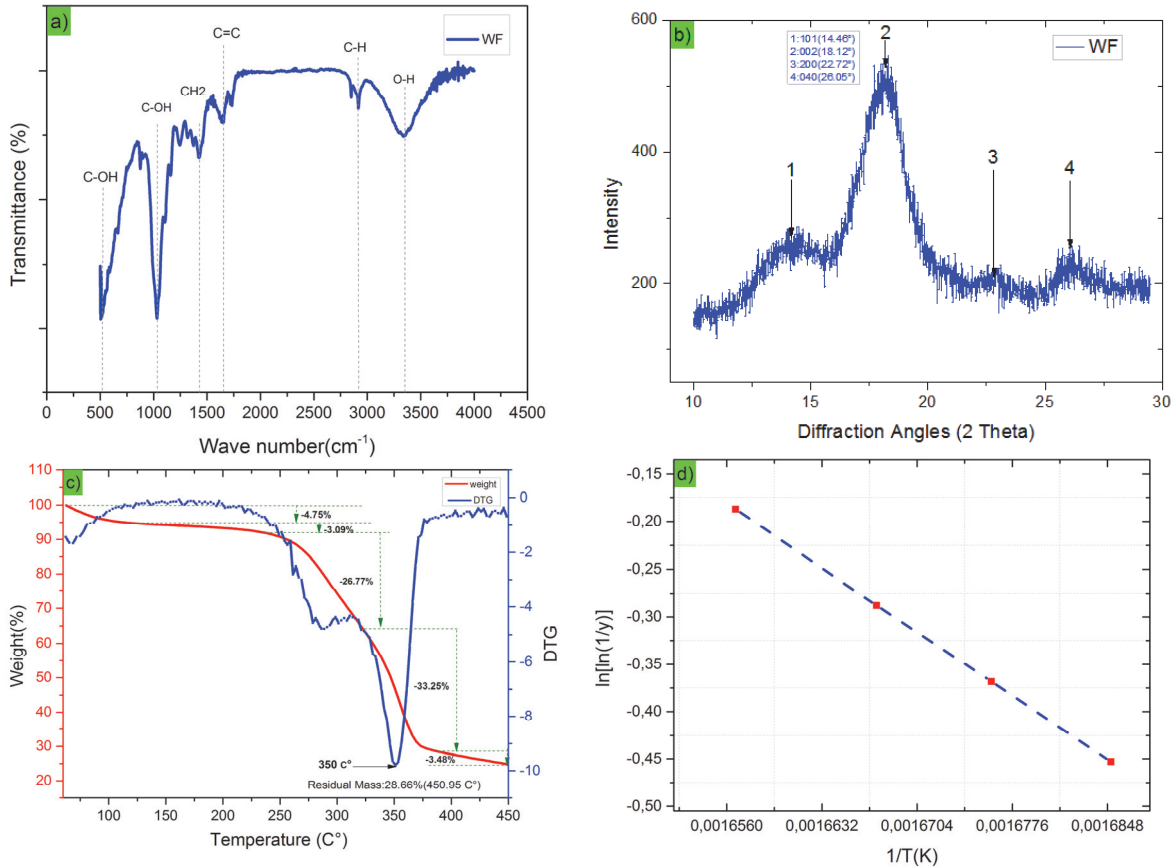

Fig.3. (a) FTIR spectra (b) XRD spectrum, (c) TG and DTG curves and (d) Broido's plot of WF fiber

Table 1. FTIR bands observed for WF fiber

Band position in this work. (cm^{-1})	Wavenumber range (cm^{-1})	Origin	Reference
3340	3600–3100	Hydrogen bonded O-H stretching	Manimaran et al. (2018)
2917	2950–2854	vibrations of the C-H aliphatic chains	Cotugno et al. (2001)
1650	1732 – 1637	the carbonyl groups (C =O) of lignin and hemicellulose	Belouadah et al. (2015)
1438	1430	CH2 symmetric bending from cellulose	Belouadah et al. (2015) ;Fiore et al. (2014), & Sgriccia et al. (2008).
1031	1035	Attributed to the C-OH stretching of lignin.	Senthamaraikannan et al. (2018) and Liu et al. (2009).
514	588	(C-OH) bending	Belouadah et al. (2015) & Rosa et al. (2010)

The spectrum band at 3340 cm^{-1} represents the stretching vibration of O-H bonds of cellulose and hemicellulose (Manimaran et al., 2018) for the cellulosic materials and it has been shown by deconvolution that this zone represents the hydrogen bonds of the inter and intra molecular network of cellulose as well as the free hydroxyl groups of hemicelluloses. The peak at 2917 cm^{-1} represents the macromolecular interactions of cellulose and hemicellulose and the presence of water in the fibers (Cotugno et al., 2001). Characteristic wave number of the lignin is located at 1650 cm^{-1} is assigned to the vibration and flexion of the water molecule (Fiore et al., 2014 ; Belouadah et al., 2015). The peak

at 1438 cm^{-1} characteristic of the carboxyl functions of the pectins constituting the middle lamella (Belouadah et al., 2015; Sgriccia et al., 2008) are also affected by water absorption. The peak at 1031 cm^{-1} is attributed to the C-OH stretch of lignin (Senthamaraikannan et al. 2018; Liu et al. 2008). The peak 514 cm^{-1} represents the flexion of (C-OH) (Belouadah et al., 2015; Rosa et al., 2010).

3.3. XRD Analysis

The WF corresponding spectrum shows five well defined peaks at the following angles: $2\theta =14.46°$, $18.12°$ et $22.67°$, $26.05°$ as shown in Fig. 3(b). The observation of a major crystalline peak of the diffraction angle $14.46°$ corresponding to the plane (1 1 0) (Dai et al., 2009), the angles $18.12°$, $22.67°$ and $26.05°$ represent the planes (1 1 0) (0 0 2) (0 0 4) respectively, which corresponds to the planar crystallographic family of cellulose (Saravanakumar et al.,2013). The crystallinity index (CrI) of the natural fibers WF is calculated according to the Segal empirical method developed by (Segal et al., 1959) by using the following Eq. (2):

$$\text{CrI}\% = \left[\frac{(I_{002} - I_{am})}{I_{002}}\right] \times 100 \tag{2}$$

where I$_{002}$ is the maximum diffraction intensity and to calculate the size of the crystallites (Cr_{size}) using Scherrer equation 3 (Troedec et al., 2008; Saravanakumar et al., 2013):

$$Cr_{size} = \left[\frac{(k\lambda)}{\beta cos\theta}\right] \times 100 \tag{3}$$

Crystallinity index (CrI) of washingtonia Filifera fiber is calculated by Eq. (2), is 48.88%, compared with other cellulosic fibers, the CrI of the WF fiber is high that that found in the, L. spartum 46.19% (Belouadah et al., 2017) and also Grewia Tilifolia (41,7%) (Jayaramudu et al., 2010), the date palm (38.5%) (Abdal-hay et al. 2012), but is lower than that found in Althaea officinalis L. (68%) (Sarikanat et al, 2012) Sansevieria cylindrica (60%) (Sreenivasan et al., 2011) ehrenbergii (52.27%) (Sathishkumar, 2013). The size of crystallite (Cr_{size}) of the WF fiber is 2.55 nm was calculated by Eq. (3) in the first crystalline peak. This value is high compared to Pergularia Tomentosa L. 2.41nm (Sakji 2016) but lower than Cissus quadrangularis stem 3.91nm (Indran & Raj, 2015) and Furcraea foetida 28.36 nm (Manimaran et al., 2018).

3.4. Thermal properties

The thermal degradation for the TG and DTG curves for the WF fiber are shown in Fig. 3(c). The first mass losses were observed are (4.75%) and (3.09%) were recorded between 116 °C et 213 °C related to the decomposition of hemicellulose and glycosidic bonds of cellulose (Indran and Raj 2015), while the polymerization of hemicelluloses for Dichrostachys Cinerea fiber recorded between 226°C and 284°C (Baskaran et al., 2018), hemicelluloses and pectins for other fibers would be degraded between 250°C and 320°C (Fiore et al., 2014 ;Yang et al., 2007), the decomposition of hemicelluloses, glycosidic bonds of cellulose was recorded between 220°C and 307°C (Belouadah et al. 2015). The third loss of weight (33.25%) between the temperature 322°C and 385°C is related to the degradation of cellulose as reported by many studies in the literature the fact that cellulose will degrade between 300 and 420C° (Fiore et al., 2014;Yang et al., 2007). For some authors the lignins would decompose around 200°C (Joseph et al. 2003) and beyond 400°C (Rosa et al., 2010). This analysis shows that the washingtonia fiber is stable up to about (201°C) but other fibers like the arundo leaf fiber is stable up to about (210°C) (Scalici et al., 2016) and artichaut (230°C) (Fiore et al., 2011). In addition, the maximum temperature for the WF fiber is about 322°C and 385°C, respectively, the thermal stability of the fiber is lower. However the percentage of residual mass found at 450°C was about 3.48% and 28.66 % respectively.

Another important parameter in the evaluation of the thermal stability of the WF fiber is the activation energy. The latter can be calculated by the method of Broido (Broido, 1969) using the following equation:

$$\ln\left[\ln\left(\frac{1}{y}\right)\right] = -\left(\frac{E_a}{R}\right)\left[\left(\frac{1}{T} + K\right)\right] \tag{4}$$

where y is the normalized weight (w_o / w_t), w_o is the initial weight and w_t is the weight at any instant t, E_a is the apparent activation energy, R is the gas universal constant (8.314 J / mol K), while T is the absolute temperature in Kelvin, K is constant. The apparent activation energy (E_a) calculated from the curve of ($\ln[\ln(1/y)]$) versus ($1/T$) is 72.46 kJ / mol (Fig. 3 (d)). This value is closer to those obtained from the thermal analysis of other natural fibers such as: Lygeum spartum L (68.44 kJ / mol) (Belouadah et al.,2015), c quadrangularis (74.18 kJ / mol) (Indran et al. 2014), P juliflora (76.72 kJ / mol) (Saravanakumar et al., 2013). The comparison between the thermal analysis parameters of the WF fiber ($T_S = 201°C$, $T_d = 350°C$, RW% = 28.66(450°C)) and other natural fiber fibers as Lygeums partum (T_S=220°C T_d=338.7°C, RW%=23.51(600°C)) (Belouadah et al., 2015), Manicaria (T_S=220°C, T_d=300-370°C, RW%=23(600°C)) (Porras et al., 2016), Prosopis juliflora bark (T_S=217°C T_d=331.1°C, RW%=21.88(1000°C)) (Saravanakumar et al., 2013). As T_S is the maximum temperature stability, T_d is the maximum temperature decomposition, RW is the residual mass.

3.5. Tensile properties of WF

The stress-strain curve (Fig. 4(a)) obtained from the static tensile tests of W. Filifera fibers, shows that they have a mechanical behavior. This behavior is characterized by an elastic linear region (e = 1%) with a very high slope followed by a nonlinear transition zone and finally by a practically linear behavior, but with a slope much lower than that of the first zone, until the abrupt rupture of the fiber. It is also important to point out that the second phase (non-linear transition zone) is sometimes characterized by discontinuities that correspond to the breakage of some microfibrils for some tested samples (Bessadok et al., 2008) interprets the appearance of these curves as the behavior of a hard material. But on the other hand, other lignocellulosic fibers represented in Table 2 show that there is a different behavior, for example, Furcraea foetida by (Manimaran et al., 2018), Artisdita hystrix by (Kathiresan et al., 2016). The WF fibers are tested under static tension, under the same conditions. Fig. 4(b) represents the distribution of the mechanical properties namely the stress and strain at break and the Young's modulus. It is clear that there is a significant dispersion in the results, this dispersion may be mainly related to several factors that affect the fiber: test conditions and parameters, plant characteristics, and fiber section measurement. With regard to the characteristics of the plant, the factors that may affect the mechanical behavior are: source of the plant, age, fiber extraction mechanisms and presence of defects in the fibers.

The results of the mechanical properties as a function of the diameter of the plant fibers studied in this work (Figs. 5 (a), 5(b) and 5(c)) are characterized by dispersions which are on one hand due to the origin of their location in the plant and also the methods of extraction of these fibers. In other words, the fibers do not have the same dimensions all along the blade, that is to say that the dimensions of the fibers are greater at the foot of the blade relative to its head and this is function of the maturation of the plant. Plots 5a, 5b and 5c may be plotted in another way as shown in Fig. 5 to show the tensile properties of the different WF fibers as a function of measurement length (LM). Tensile tests of a single plant fiber are difficult to achieve because of the very small diameter (of the order of 0.3 mm) and to analyze because of the large recorded dispersion. This variability can be explained by the distribution of defects in the fiber or on the surface of the fiber (Silva et al., 2008) and it is therefore necessary to use statistical approaches.

Table 2. Comparison of physical, chemical, crystalline, thermal and tensile properties of WFs with various natural fibers

|	Physical properties		Thermal Properties		Crystalline properties		Tensile properties				Reference
	Diameter (µm)	Density (Kg/m³)	Thermal Stability (°C)	Maximum degradation temperature (°C)	CI(%)	CS(nm)	Tensile Strength (MPa)	Young's Modulus (GPa)	Elongation at break(%)	Microfibril Angle(°)	
Washingtonia Filifera(WF)	**252 ± 46**	**1.07-1.12**	**201**	**350**	**48.8**	**2.55**	**134 ± 83**	**2.17± 1.05**	**26.55 ± 8.24**	**41**	**Present Work**
Furcraea foetida	12.8	778	-	320.5	52.6	28.36	623.52± 45	6.52 ± 1.9	10.32 ± 1.6	-	Manimaran et al, (2018)
Saharanaloe vera	80.61	1325.1	225	350	56.5	5.72	805.5	42.29	2.39	11.1	Balaji, & Nagarajan (2017)
Pennisetum purpureum	210–270	-	230	364.7	-	-	73 ± 6	5.68 ± 0.14	1.40 ± 0.23	-	(Ridzuan et al., 2016)
Artisdita hystrix	-	540	-	298.8	44.85	-	440±13.4	1.57± 0.04	-	12.64±0.45	Kathiresan et al.,(2016)
Cissus quadrangularis stem	770-870	1220	270	342.1	47.15	3.91	2300- 5479	56-234	3.75-11.14	4.95 ± 0.32	Indran et al,(2015)
Lygeum spartum L	180–433	1499.7±3.1	220	338.7	46.19	-	64.63-280	4.47–13.27	1.49–3.74	12.65° ±2.85	Belouada et al.,(2015)
Manicaria saccifera palm	-	840-1070	220	370	-	-	72.09±15	2.20 ± 0.44	-	-	Porras et al.,(2015)
Arundo Donax	-	1168	275	320	-	-	248	9.4	3.24	6.85± 1.23	Fiore et al.,(2014)
Cissus quadrangularis root	610–725	1510		328.9	56.6	7.04	1857-5330	68-230	3.57–8.37		Indran et al.(2014)
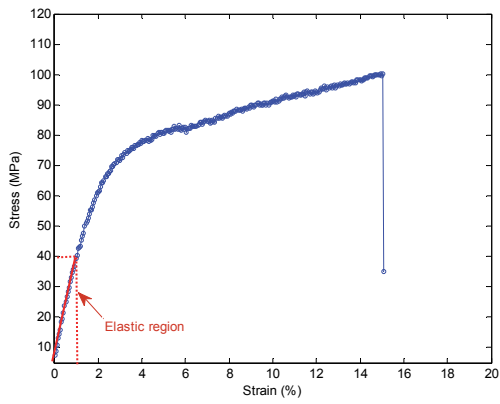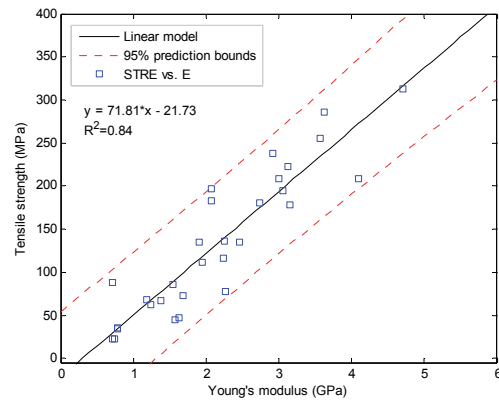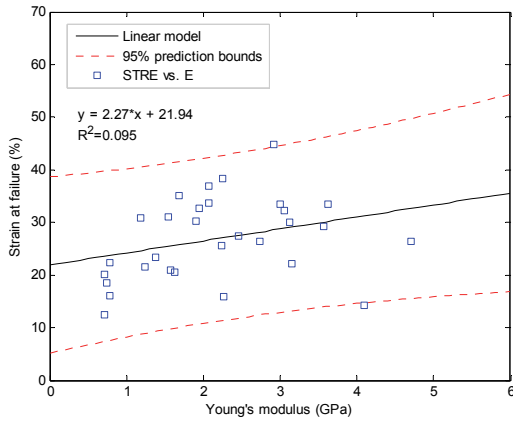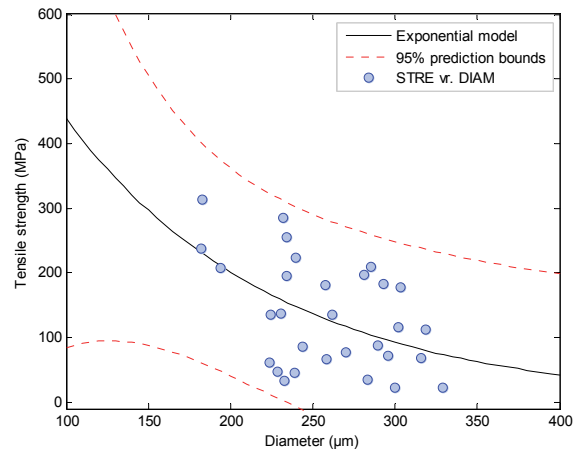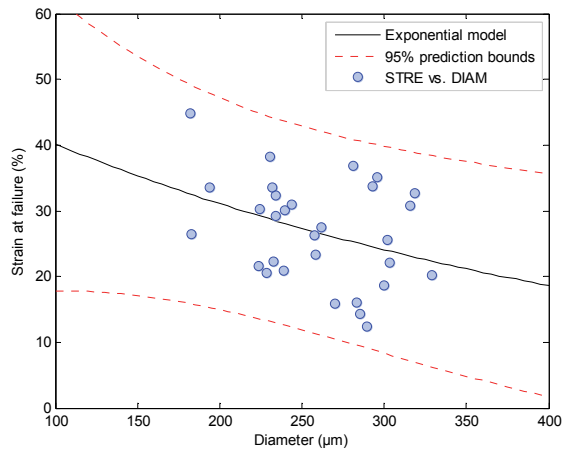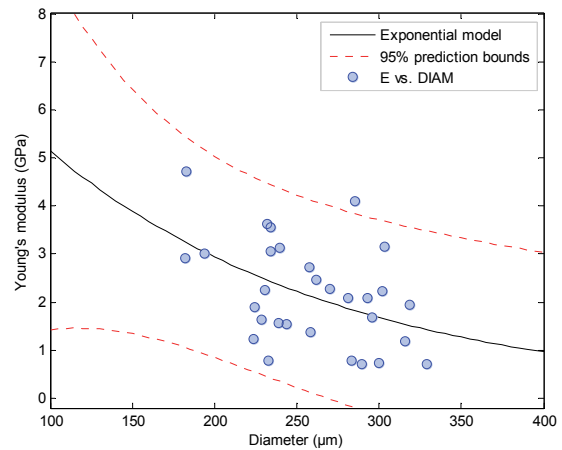
Fig.4. (a) Typical stress–strain curve for Washingtonia Filifera fiber, (b, c) tensile strength and strain at failure vs. Young's modulus for all tests of the WF fibers
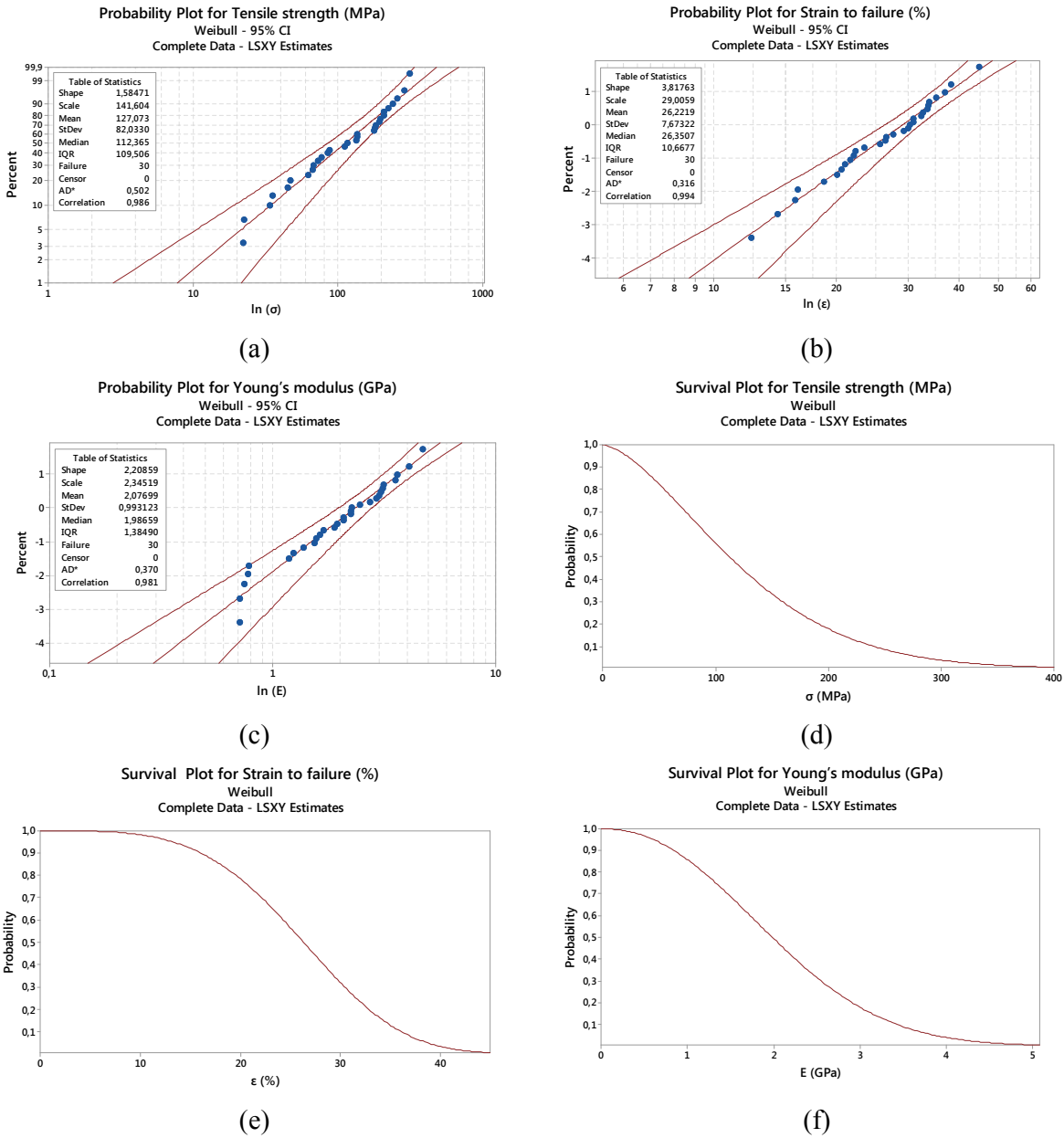
Probability Plot for Tensile strength (MPa)
Weibull - 95% CI
Complete Data - LSXY Estimates

Table of Statistics
Shape 1,58471
Scale 141,604
Mean 127,073
StDev 82,0330
Median 112,365
IQR 109,506
Failure 30
Censor 0
AD* 0,502
Correlation 0,986

(a)

Probability Plot for Strain to failure (%)
Weibull - 95% CI
Complete Data - LSXY Estimates

Table of Statistics
Shape 3,81763
Scale 29,0059
Mean 26,2219
StDev 7,67322
Median 26,3507
IQR 10,6677
Failure 30
Censor 0
AD* 0,316
Correlation 0,994

(b)

Probability Plot for Young's modulus (GPa)
Weibull - 95% CI
Complete Data - LSXY Estimates

Table of Statistics
Shape 2,20859
Scale 2,34519
Mean 2,07699
StDev 0,993123
Median 1,98659
IQR 1,38490
Failure 30
Censor 0
AD* 0,370
Correlation 0,981

(c)

Survival Plot for Tensile strength (MPa)
Weibull
Complete Data - LSXY Estimates

(d)

Survival Plot for Strain to failure (%)
Weibull
Complete Data - LSXY Estimates

(e)

Survival Plot for Young's modulus (GPa)
Weibull
Complete Data - LSXY Estimates

(f)

Fig. 5. (a, b, c) Two Weibull distribution and (d, e, f) Probability of survival graphs for the tensile strength, strain at break, and Young's modulus of the WF fibers

In order to evaluate its average mechanical properties, the statistical analysis of the experimental data obtained from the uni-axial tensile tests performed for the fibers presented in this work are processed using the Minitab 16 software with the two parameter Weibull model used by several authors for different lignocellulosic fibers, (Fiore et al., 2014), to estimate their mechanical properties. The cumulative distribution function of the two-parameter Weibull model is defined by the flowing expression:

$$F(x) = 1 - \text{Exp}\left[-\left(\frac{x}{s}\right)^m\right]$$
(5)

where *x*, *s* and *m* are all real positives, *s* being the threshold that represent an average value of the parameter *x* and *m* is the shape parameter or the Weibull module. Fig. 5 shows the variation of the average mechanical properties, tensile strength and strain at failure, respectively, as function of the mean values of the Young's modulus. The linear model of prediction gives a level of confidence equal to 95% (5% error) for the different series of tests performed in this work. The relationship between Young's modulus and breaking stress (Fig. 5(b, c)) is that when the stress increases, Young's modulus decreases. Similarly, for the strain as function of Young's modulus (Fig. 5(c)).

4. Conclusions

In this paper, the properties of a new lignocellulosic fiber extracted from the Washingtonia Filifera. (WF) plant were studied in order to evaluate the possibility of using it as reinforcement in composite biomaterials. The following conclusions were drawn from the results of the physicochemical, mechanical and thermal characterization of this new natural fiber.

- ➢ XRD analysis showed the semi-crystalline nature of the WF fiber.
- ➢ The FTIR spectrum bands obtained for the WF fiber were analyzed and compared to those reported in the literature for other lignocellulosic fibers.
- ➢ Crystallinity index (CrI) of Washingtonia Filifera fiber is 48.88%, compared with other cellulosic fibers. Crystallite size of WF fiber is 2.55 nm in the first lens peak.
- ➢ Thermogravimetric analysis of the WF fiber has shown a thermal stability up to 201°C, which confirms the possibility of its use as reinforcement for composite materials.
- ➢ The mechanical properties resulting from the monotonic tensile tests carried out on the WF fibers give a strength modulus of 134 ± 83 MPa, a strain at break of $26.55 \pm 8.24\%$ and Young's modulus of 2.17 ± 1.05 GPa, and show that these values are globally similar, to other plant fibers.
- ➢ The analysis of the results of the tensile tests showed that the manufacturing characteristics estimated by LS-Weibull with 2 parameters are close to those obtained experimentally.

References

Abdal-hay, A., Suardana, N. P. G., Jung, D. Y., Choi, K.-S., & Lim, J. K. (2012). Effect of diameters and alkali treatment on the tensile properties of date palm fiber reinforced epoxy composites. *International Journal of Precision Engineering and Manufacturing, 13*(7), 1199–1206.

Aliha, M. R. M., Razmi, A., & Mansourian, A. (2017). The influence of natural and synthetic fibers on low temperature mixed mode I+ II fracture behavior of warm mix asphalt (WMA) materials. *Engineering Fracture Mechanics, 182*, 322-336.

Azwa, Z. N., Yousif, B. F., Manalo, A. C., & Karunasena, W. (2013). A review on the degradability of polymeric composites based on natural fibers. *Materials and Design, 47*, 424–442.

Baskaran, P. G., Kathiresan, M., Senthamaraikannan, P., & Saravanakumar, S. S. (2018). Characterization of New Natural Cellulosic Fiber from the Bark of Dichrostachys Cinerea. *Journal of Natural Fibers, 15*(1), 62–68.

Beakou, A., Ntenga, R., Lepetit, J., Ateba, J. A., & Ayina, L. O. (2008). Physico-chemical and microstructural characterization of "Rhectophyllum camerunense" plant fiber. *Composites Part A: Applied Science and Manufacturing, 39*(1), 67–74.

Belouadah, Z., Ati, A., & Rokbi, M. (2015). Characterization of new natural cellulosic fiber from Lygeum spartum L. *Carbohydrate Polymers, 134*, 429–437.

Bessadok, A., Marais, S., Roudesli, S., Lixon, C., & Métayer, M. (2008). Influence of chemical modifications on water-sorption and mechanical properties of Agave fibers. Composites Part A: *Applied Science and Manufacturing, 39*(1), 29–45.

Bouakba, M., Issasfa B., Boukatem M. & Belloufi A. (2016). Effect of fiber volume fraction in the tensile properties of renewable Diss fiber /polyester composite. *Engineering Solid Mechanics, 4*, 91–96.

Bouakba, M., Bezazi, A., Boba, K., Scarpa, F.& Bellamy, S. (2013). Cactus fiber/polyester composite: Manufacturing, quasi-static mechanical and fatigue characterization. *Composites Science and Technology, 74*, 150–159.

Cotugno, S., Larobina, D., Mensitieri, G., Musto, P., & Ragosta, G. (2001). A novel spectroscopic approach to investigate transport processes in polymers: The case of water-epoxy system. *Polymer, 42*(15), 6431–6438.

Dai, D., & Fan, M. (2010). Characteristic and performance of elementary hemp fiber. *Materials Sciences and Applications, 1*(06), 336.

De Rosa, I. M., Kenny, J. M., Puglia, D., Santulli, C., & Sarasini, F. (2010). Morphological, thermal and mechanical characterization of okra (Abelmoschus esculentus) fibers as potential reinforcement in polymer composites. *Composites Science and Technology, 70*(1), 116–122.

Fiore, V., Scalici, T., & Valenza, A. (2014). Characterization of a new natural fiber from Arundo donax L. as potential reinforcement of polymer composites. *Carbohydrate Polymers, 106*(1), 77–83.

Fiore, V., Valenza, A., & Di Bella, G. (2011). Artichoke (Cynara cardunculus L.) fibers as potential reinforcement of composite structures. *Composites Science and Technology, 71*(8), 1138–1144.

Guo, C., Zhou, L., & Lv, J. (2013). Effects of expandable graphite and modified ammonium polyphosphate on the flame-retardant and mechanical properties of wood flour-polypropylene composites. *Polymers and Polymer Composites, 21*(7), 449–456.

Ibrahim, M. M., Dufresne, A., El-Zawawy, W. K., & Agblevor, F. A. (2010). Banana fibers and microfibrils as lignocellulosic reinforcements in polymer composites. *Carbohydrate Polymers, 81*, 811–819.

Indran, S., & Raj, R. E. (2015a). Characterization of new natural cellulosic fiber from Cissus quadrangularis stem. *Carbohydrate Polymers, 117*, 392–399.

Indran, S., Raj, R. E., & Sreenivasan, V. S. (2014). Characterization of new natural cellulosic fiber from Cissus quadrangularis root. *Carbohydrate Polymers, 110*, 423–429.

Ishak, M. R., Sapuan, S. M., Leman, Z., Rahman, M. Z. A., Anwar, U. M. K., & Siregar, J. P. (2013). Sugar palm (Arenga pinnata): Its fibers, polymers and composites. *Carbohydrate Polymers, 91*(2), 699–710.

Jawaid, M., & Abdul Khalil, H. P. S. (2011). Cellulosic/synthetic fiber reinforced polymer hybrid composites: A review. *Carbohydrate Polymers, 86*(1), 1–18.

Jayaramudu, J., Guduri, B. R., & Rajulu, A. V. (2010). Characterization of new natural cellulosic fabric Grewia tilifolia. *Carbohydrate Polymers, 79*(4), 847–851.

Joseph, P. V, Joseph, K., Thomas, S., Pillai, C. K. S., Prasad, V. S., Groeninckx, G., & Sarkissova, M. (2003). The thermal and crystallisation studies of short sisal fiber reinforced polypropylene composites. *Composites Part A: Applied Science and Manufacturing, 34*(3), 253–266.

k, H., Dufresne, A., Khelifi, B., Bendahou, A., Taourirte, M., Raihane, M., … Sami, N. (2006). Short palm tree fibers-Thermoset matrices composites. *Composites Part A Applied Science and Manufacturing, 37*(9), 1413–1422.

Keller, A. (2003). Compounding and mechanical properties of biodegradable hemp fiber composites. *Composites Science and Technology, 63*(9), 1307–1316.

Le Troedec, M., Sedan, D., Peyratout, C., Bonnet, J. P., Smith, A., Guinebretiere, R., …, & Krausz, P. (2008). Influence of various chemical treatments on the composition and structure of hemp fibers. *Composites Part A: Applied Science and Manufacturing, 39*(3), 514–522.

Liu, D., Han, G., Huang, J., & Zhang, Y. (2009). Composition and structure study of natural Nelumbo nucifera fiber. *Carbohydrate Polymers, 75*(1), 39–43.

Liu, J., Xue, Z., Zhang, W., Yan, M., & Xia, Y. (2018). Preparation and properties of wet-spun agar fibers. Carbohydrate Polymers 181, 760 (2018).

Manimaran, P., Senthamaraikannan, P., Murugananthan, K., & Sanjay, M. R. (2018). Physicochemical Properties of New Cellulosic Fibers from Azadirachta indica Plant. *Journal of Natural Fibers, 15*(1), 29–38.

Manimaran, P., Senthamaraikannan, P., Sanjay, M. R., Marichelvam, M. K., & Jawaid, M. (2018). Study on characterization of Furcraea foetida new natural fiber as composite reinforcement for lightweight applications. *Carbohydrate Polymers, 181*, 650–658.

Porras, A., Maranon, A., & Ashcroft, I. A. (2016). Thermo-mechanical characterization of manicaria saccifera natural fabric reinforced poly-lactic acid composite lamina. *Composites Part A: Applied Science and Manufacturing, 81*, 105–110.

Reddy, K. O., Maheswari, C. U., Dhlamini, M. S., Mothudi, B. M., Kommula, V. P., Zhang, J., Rajulu, A. V. (2018). Extraction and characterization of cellulose single fibers from native african napier grass. *Carbohydrate Polymers, 188*, 85–91.

Ridzuan, M. J. M., Abdul Majid, M. S., Afendi, M., Aqmariah Kanafiah, S. N., Zahri, J. M., & Gibson, A. G. (2016). Characterisation of natural cellulosic fiber from Pennisetum purpureum stem as potential reinforcement of polymer composites. *Materials and Design, 89*, 839–847.

Sakji, N., Jabli, M., Khoffi, F., Tka, N., Zouhaier, R., Ibala, W., Durand, B. (2016). Physico-chemical characteristics of a seed fiber arised from Pergularia Tomentosa L. *Fibers and Polymers, 17*(12), 2095–2104.

Sandeep, N. C., Raghavendra Rao, H., & Hemachandra Reddy, K. (2017). Extraction and Characterization of Physicochemical and Tensile Properties of Aegle Marmelos fiber. *Materials Today: Proceedings, 4*(2), 3158–3165.

Saravanakumar, S. S., Kumaravel, A., Nagarajan, T., Sudhakar, P., & Baskaran, R. (2013). Characterization of a novel natural cellulosic fiber from Prosopis juliflora bark. *Carbohydrate Polymers, 92*(2), 1928–1933.

Sarikanat, M., Seki, Y., Sever, K., & Durmus, C. (2014). Determination of properties of Althaea officinalis L. (Marshmallow) fibers as a potential plant fiber in polymeric composite materials. *Composites Part B: Engineering, 57*, 180–186.

Sathishkumar, T. P., Navaneethakrishnan, P., Shankar, S., & Rajasekar, R. (2013). Characterization of new cellulose sansevieria ehrenbergii fibers for polymer composites. *Composite Interfaces, 20*(8), 575–593.

Scalici, T., Fiore, V., & Valenza, A. (2016). Effect of plasma treatment on the properties of Arundo Donax L. leaf fibers and its bio-based epoxy composites: A preliminary study. *Composites Part B: Engineering, 94*, 167–175.

Segal, L., Creely, J. J., Martin, A. E., & Conrad, C. M. (1959). An Empirical Method for Estimating the Degree of Crystallinity of Native Cellulose Using the X-Ray Diffractometer. *Textile Research Journal, 29*(10), 786–794.

Senthamaraikannan, P., & Kathiresan, M. (2018). Characterization of raw and alkali treated new natural cellulosic fiber from Coccinia grandis.L. *Carbohydrate Polymers, 186*, 332–343.

Sgriccia, N., Hawley, M. C., & Misra, M. (2008). Characterization of natural fiber surfaces and natural fiber composites. *Composites: Part A, 39*(10), 1632–1637.

Silva, F. de A., Chawla, N., & Filho, R. D. de T. (2008). Tensile behavior of high performance natural (sisal) fibers. *Composites Science and Technology, 68*(15–16), 3438–3443.

Sreenivasan, V. S., Ravindran, D., Manikandan, V., & Narayanasamy, R. (2011). Mechanical properties of randomly oriented short Sansevieria cylindrica fiber/polyester composites. *Materials & Design, 32*(4), 2444–2455.

Suryanto, H., Marsyahyo, E., Irawan, Y. S., & Soenoko, R. (2013). Effect of Alkali Treatment on Crystalline Structure of Cellulose Fiber from Mendong. *Engineering Materials, 594–595*, 720–724.

Teixeira, E. D. M., Pasquini, D., Curvelo, A. A. S., & Corradini, E. (2009). Author's personal copy Cassava bagasse cellulose nanofibrils reinforced thermoplastic cassava starch. *Carbohydrate Polymers Journal, 78*, 422–431.

Thomason, J. L., Carruthers, J., Kelly, J., & Johnson, G. (2011). Fiber cross-section determination and variability in sisal and flax and its effects on fiber performance characterisation. *Composites Science and Technology, 71*(7), 1008–1015.

Yang, H., Yan, R., Chen, H., Lee, D. H., & Zheng, C. (2007). Characteristics of hemicellulose, cellulose and lignin pyrolysis. *Fuel, 86*(12–13), 1781–1788.